*J. agric. Engng Res.* (1996) **63,** 93–102

# Forecasting Earth Surface Temperature for the Optimal Application of Frost Protection Methods

B. Krasovitski; E. Kimmel; I. Amir

Department of Agricultural Engineering, Technion, Haifa 32000, Israel

*(Received 2 January 1995; accepted in revised form 23 August 1995)*

A method is presented which predicts when the earth surface temperature will fall below a safe threshold for plants during a night of frost. The method requires as an input a set of earth surface temperatures which ought to be measured soon after sunset. Unknown parameters of the heat transfer process in the soil and the air are determined by an optimization procedure. Based on these parameters, the evolution of earth surface temperature is predicted for the rest of the night. Simulation experiments show good quality of the prediction.



## 1. Introduction

Radiative frost conditions cause considerable damage to crops all over the world. The main cause of the damage is the excessive cooling of the plant surfaces and subsequent freezing of the plant cells, due to radiative heat flux to the atmosphere. This happens during a clear night when there is no wind, no clouds, and the air humidity is low.[1,2] In order to prevent damage to the plants, several protective methods are available such as fogging, wetting the soil and the plants, and covering techniques using plastic, paper or foam.[3–6]

### Notation

| | |
|---|---|
| $T$ | temperature, °C |
| $\tilde{T}$ | absolute temperature, K |
| $\lambda$ | heat conductivity, W/m K |
| $c$ | specific heat |
| $\kappa$ | heat diffusivity, $m^2/s$ |
| $h_g$ | depth of daily temperature perturbation zone, m |
| $x$ | vertical coordinate, m |
| $h$ | thickness of layer, m |
| $R$ | thickness of temperature perturbation layer, m |
| $a$ | coefficient in temperature profile polynomial |
| b | vector of unknown parameters |
| $\beta$ | unknown parameter |
| $M$ | number of parameters |
| $J$ | deviation functional |
| $S$ | functional gradient absolute value |
| $\sigma$ | Stefan–Boltzmann constant, $W/m^2\ K^4$ |
| $p$ | partial pressure of water vapour in atmosphere, mm Hg |
| $\phi$ | measured earth surface temperature, °C |
| $L$ | number of measurements |
| $N$ | number of measurement points over field |
| $X$ | sensitivity coefficient |
| $\tau$ | time, s |
| $\tau_f$ | moment when earth surface temperature falls to critical level, h |

$$\prod_{j=1}^{M} a_j \equiv a_1 \times a_2 \times \cdots a_M$$

*Subscripts*

| | |
|---|---|
| a | air |
| g | ground |
| 0 | initial (or natural) condition |
| f | final |
| s | earth surface |
| A | air (far from inversion layer) |
| e | evaluated value |
| t | true value |

For effective application of the protection system, a reliable method is needed that will indicate whether frost is expected and at which moment to start applying the protective means, when frost is forecast. The forecast of the coming frost must provide the



0021-8634/96/020093 + 09 $18.00/0

farmer with sufficient time to prepare and apply means of frost protection.

Forecasting based on known computation techniques is hampered by lack of information about the values of the parameters used in the mathematical description of the problem. The prediction method presented in this paper is based on measurements of earth surface temperature during the initial phase of night cooling and on an approximate solution of the heat transfer problem for the upper layer of the soil during a night of frost. The developed method provides the parameters for the heat transfer model, and this provides a basis for a method of forecasting earth surface temperature.

## 2. Heat transfer model

During the night, the upper earth layer cools down because of infrared radiation loss from the earth's surface. This radiation loss is derived from the difference between the Stefan–Boltzmann radiation from the earth's surface and the counter radiation from the atmosphere, which depends on air temperature, water vapour content, carbon dioxide and ozone concentrations, and cloudiness. Since the ratio of carbon dioxide and ozone in the atmosphere are essentially constant, the intensity of night radiation loss depends mostly on water vapour content and air temperature. Heat fluxes between the upper earth layer and adjacent air and the earth underlayers also contribute to the heat balance of the earth surface.

At the beginning of a night of frost, the air and soil vertical temperature profiles near the earth surface can be assumed uniform. This is related to the inversion of the temperature profile which occurs shortly before or after sunset.[5] Confirmation of this assumption is obtained from measurements of air and ground temperature which show uniformity of temperature distribution in the air adjacent to the earth surface and in the upper layer of the ground (*Figs 1* and *2*, Ref. 7). As can be seen from these figures, the temperature distributions of the upper layer of the earth and the lower layer of air at inversion (about 1800 hrs) are uniform. Here we should take into account, that these measurements related to different experiments and therefore values of the earth and air temperatures at the inversion moment are different.

We assume that all environmental and geometrical parameters are uniform in the horizontal direction, and that the heat flux from the earth surface to the adjacent air is negligible when the inversion layer appears.

Taking into consideration the above facts, a one-dimensional heat transfer model for a flat earth layer is developed. A schematic description of the problem is shown in *Fig. 3*.

The heat transfer equation for the earth layer is

$$\frac{\partial T_g}{\partial \tau} = \kappa_g \frac{\partial^2 T_g}{\partial x^2} \quad 0 \leqslant x \leqslant h_g \tag{1}$$

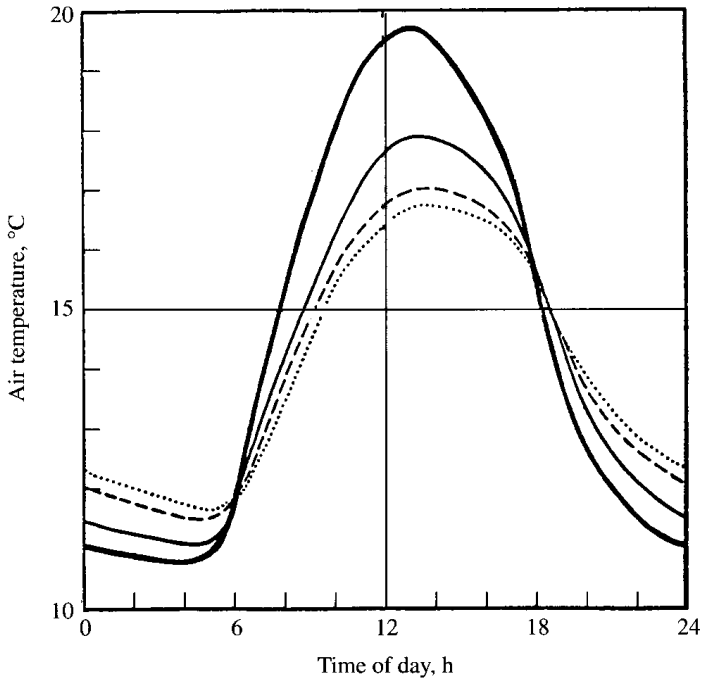


*Fig. 1. Daily course of air temperature at the different heights above the ground (· · · · · 17·1 m; – – – 7·1 m; —— 1·2 m; —— 2·5 cm)*

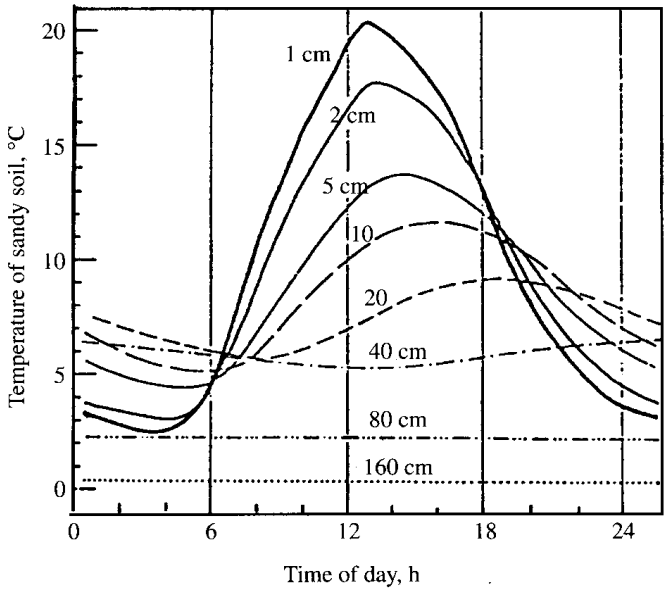


*Fig. 2. Daily course of the earth temperature at given depths*

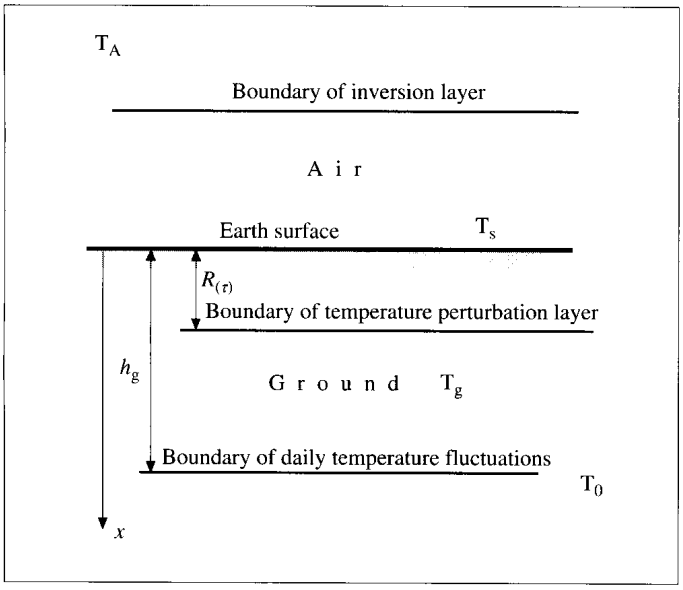


*Fig. 3. A schematic presentation of the problem. $h_g$ depth of soil layer where daily variations of temperatures occur; R thickness of temperature perturbation layer; $T_0$ the natural temperature of the soil at a depth of the daily temperature perturbation zone; $T_A$ the air temperature far from the inversion layer; $T_s$ earth surface temperature; $T_g$ ground temperature*

where $h_g$ denotes the depth of soil layer where daily variations of temperatures occur.

The initial and boundary conditions are as follows.

Initial condition

$$T_g = T_0 \quad \text{at} \quad \tau = \tau_0; \quad x \geqslant 0 \tag{2}$$

Boundary conditions

$$T_g = T_0 \quad \text{at} \quad x = h_g; \quad \tau \geqslant \tau_0 \tag{3}$$

$$\lambda_g \frac{\partial T_g}{\partial x} = \sigma[\tilde{T}_g^4 - \tilde{T}_A^4 + (A - B \times 10^{-\gamma p})] \qquad \text{at } x = 0 \tag{4}$$

Here $T_0$ is the natural temperature of the soil at the depth of the daily temperature perturbation zone; $T_A$ the air temperature far from the inversion layer; $\tilde{T} \equiv T + 273$ (absolute temperature); $\lambda_g$ heat conductivity of the soil; $\kappa_g$ heat diffusivity of the soil; $p$ partial pressure of water vapour in the atmosphere.

The right hand side of Eqn (4) accounts for the net radiative heat flux, where $A$, $B$ and $\gamma$ are empirical coefficients. In accordance with experimental data,[7-9] the coefficients are set equal to the following values: $A = 0{\cdot}82$, $B = 0{\cdot}25$, and $\gamma = 0{\cdot}126$. The value of $T_A$, which represents the air temperature far from the inversion layer,[7] may be acquired from meteorological data.

## 3. Determination of parameters

The method of solving the above set of equations (1 to 4) was developed by Krasovitski *et al.*[10] This method provides the temperature regime at the earth surface, once all the parameters used in the problem description are known. In particular, we must determine $T_0$, $T_A$, $\lambda_g$, $\kappa_g$ and $p$.

All the above parameters are hard to determine since they represent values averaged in time and space. For instance, the soil heat transfer properties ($\lambda_g$ and $\kappa_g$) are affected by soil type and moisture level and thus may vary substantially depending on location in the field and with time owing to varying weather conditions.

A prediction method is presented which is based on a set of measurements of soil surface temperature $\phi_{ni}$, taken at $L$ time points $\tau = \tau_i$ $(i = 1, 2, \ldots, L)$ at the location $n$ over the field $(n = 1, 2, \ldots, N)$. These measurements should be taken during the evening at the early phase of a night of frost after the soil temperature has fallen below a certain value. These data are used to estimate the unknown parameters and then, using our technique as described in Ref. 10, Eqns (1) to (4) are solved to provide a forecast of soil temperature for the rest of the night.

The main object of this procedure is to predict the point in time, $\tau_f$, when the earth surface temperature will fall below some critical value. In this study we choose the threshold to be 0°C.

Let us define a functional

$$J(\mathrm{b}) = \sum_{n=1}^{N} \int_{\tau_1}^{\tau_L} [T_s(\mathrm{b}, \tau) - \phi_n(\tau)]^2 d\tau \tag{5}$$

which represents in time and space the deviation of the forecast earth surface temperatures from the measured ones. Here, the interpolation functions, $\phi_n(\tau)$ are calculated for the measured earth surface temperatures at location $n$ over the field $(n = 1, 2, \ldots, N)$. They transform the discrete data into continuous functions, and are defined by

$$\phi_n(\tau) = \phi_{n,i} + (\phi_{n,i+1} - \phi_{n,i})(\tau - \tau_i)/(\tau_{i+1} - \tau_i)$$

$$\text{for} \quad \tau_i \leqslant \tau \leqslant \tau_{i+1}$$

The vector $\mathrm{b} = \{\beta_1, \beta_2, \ldots, \beta_M\}$ is the vector of unknown parameters of the problem as described by Eqns (1) to (4).

We denote the earth surface temperature, when calculated by solving Eqns (1) to (4) for a given value of b, as $T_s(\mathrm{b}, \tau)$. Obviously, the best approximation of the measured data $\phi_n(\tau)$ should be accompanied by

the minimal value of the functional $J$, which is associated with the conditions,

$$\frac{\partial J}{\partial \beta_j} = 0 \quad \text{for} \quad j = 1, 2, \ldots, M \tag{6}$$

By substituting into Eqn (6) the expression for $J$ [Eqn (5)], one gets

$$\begin{aligned}\frac{\partial J}{\partial \beta_j} &= \frac{\partial}{\partial \beta_j} \sum_{n=1}^{N} \int_{\tau_1}^{\tau_L} [T_s(b, \tau) - \phi_n(\tau)]^2 d\tau \\ &= \sum_{n=1}^{N} \int_{\tau_1}^{\tau_L} \frac{\partial}{\partial \beta_j} [T_s(b, \tau) - \phi_n(t)]^2 d\tau \\ &= \sum_{n=1}^{N} \int_{\tau_1}^{\tau_L} 2[T_s(b, \tau) - \phi_n(\tau)] \frac{\partial T_s}{\partial \beta_j} d\tau\end{aligned}$$

After denoting $\frac{\partial T_s}{\partial \beta_j}$ as $X_j$, we get the following $M$ equations

$$\sum_{n=1}^{N} \int_{\tau_1}^{\tau_L} [T_s(b, \tau) - \phi_n(\tau)] X_j(\tau) d\tau = 0, \text{ for } j = 1, 2, \ldots, M \tag{7}$$

where $X_j$ are the sensitivity coefficients.[11]

Each of the $M$ integrals in Eqns (7) may be approximated by the following sums

$$\sum_{n=1}^{N} \sum_{i=2}^{L} (\bar{T}_{si} - \bar{\phi}_{n,i}) \bar{X}_{j,i} \Delta\tau_i = 0, \qquad j = 1, 2, \ldots, M \tag{8}$$

where

$$\bar{T}_{si} = \frac{T_s(b, \tau_i) + T_s(b, \tau_{i-1})}{2}; \qquad \bar{\phi}_{n,i} = \frac{\phi_n(\tau_i) + \phi_n(\tau_{i-1})}{2}$$

$$\bar{X}_{j,i} = \frac{X_j(b, \tau_i) + X_j(b, \tau_{i-1})}{2}; \quad \Delta\tau_i = \tau_i - \tau_{i-1}$$

The system of equations (8) consists of $M$ non-linear algebraic equations for $M$ unknown parameters $\beta_1, \beta_2, \ldots, \beta_M$. The Gauss method[11] enables the non-linear set of equation to be reduced to a linear set. This is achieved by an iterative procedure which determines the $m+1$ approximation, $b_{m+1}$ from a previous m approximation, $b_m$.

For a given vector $b_m$, the corresponding temperature distribution $\bar{T}_{si}$ can be found from the solution of Eqns (1)–(4) as described later in Section 4. Next, using the first term of a Taylor series, we can relate $\bar{T}_{si}(b_{m+1})$ and $\bar{T}_{si}(b_m)$

$$\bar{T}_{si}(b_{m+1}) = \bar{T}_{si}(b_m) + \sum_{r=1}^{M} \bar{X}_{r,i}(b_m)(\beta_{r,m+1} - \beta_{r,m}) \tag{9}$$

By substituting Eqn (9) into Eqns (8), a linear set of algebraic equations is obtained for the variables $\beta_{j,m+1}$

$$\sum_{r=1}^{M} g_{j,r} \beta_{r,m+1} = a_j, \quad \text{for } j = 1, 2, \ldots, M \tag{10}$$

where

$$g_{j,r} = N \times \sum_{r=1}^{M} \sum_{i=2}^{L} \bar{X}_{j,i}(b_m) \bar{X}_{r,i}(b_m) \Delta\tau_i;$$

$$a_j = \sum_{n=1}^{N} \sum_{i=2}^{L} \bar{X}_{j,i}[-\bar{T}_{si}(b_m) + \bar{\phi}_{n,i} + \sum_{r=1}^{M} \bar{X}_{r,i}(b_m)\beta_{r,m}] \cdot \Delta\tau_i.$$

From Eqn (10) we determine the approximation $(m+1)$ of the vector b once the approximation m is known.

The procedure starts by choosing $b_0$—a "zero approximation" for the vector b. The components of this vector $\{\beta_{0,0}, \beta_{1,0}, \ldots, \beta_{M,0}\}$ are determined by means of available reference data.

This iterative procedure converges when for any $\varepsilon$ we can find an m which satisfies the following condition

$$\sum_{r=1}^{M} \left| \frac{\beta_{r,k+1} - \beta_{r,k}}{\beta_{r,k}} \right| \leqslant \varepsilon, \quad \text{for} \quad k \geqslant m. \tag{11}$$

When $\varepsilon$ equals the permissible error, we can consider $b_{m+1}$ as the approximate solution of Eqn (10) and the components of this vector are the sought parameters. The method for calculating the temperature evolution by means of these parameters is described later in Section 4.

The above described method is named by us as the "Gaussian identification procedure".

A computer program, implementing the Gaussian identification procedure, was developed. In this case we considered five unknown parameters: $\beta_1 = \tau_0$, $\beta_2 = T_A$, $= \lambda_g$, $\beta_4 = \kappa_g$, and $\beta_5 = p$. Some results, obtained while using this techniques, are discussed in Section 5.

This procedure can be improved by adding to the five unknown parameters, listed above, a sixth parameter, $\beta_6 = \tau_0$ which is the moment at which night radiative cooling begins. The addition of this unknown parameter should improve the prediction significantly since the temperature at a given time is influenced by, among other parameters, the value of $\tau_0$.

However, it is difficult to determine its value from measurements. Even if we have a set of measurements of earth surface temperature which decrease with time, it is not an easy task to find the precise starting point of this process. This difficulty is further compounded by the fact that the transition from day to night conditions does not occur at an exact point in time but is spread over an extended period.

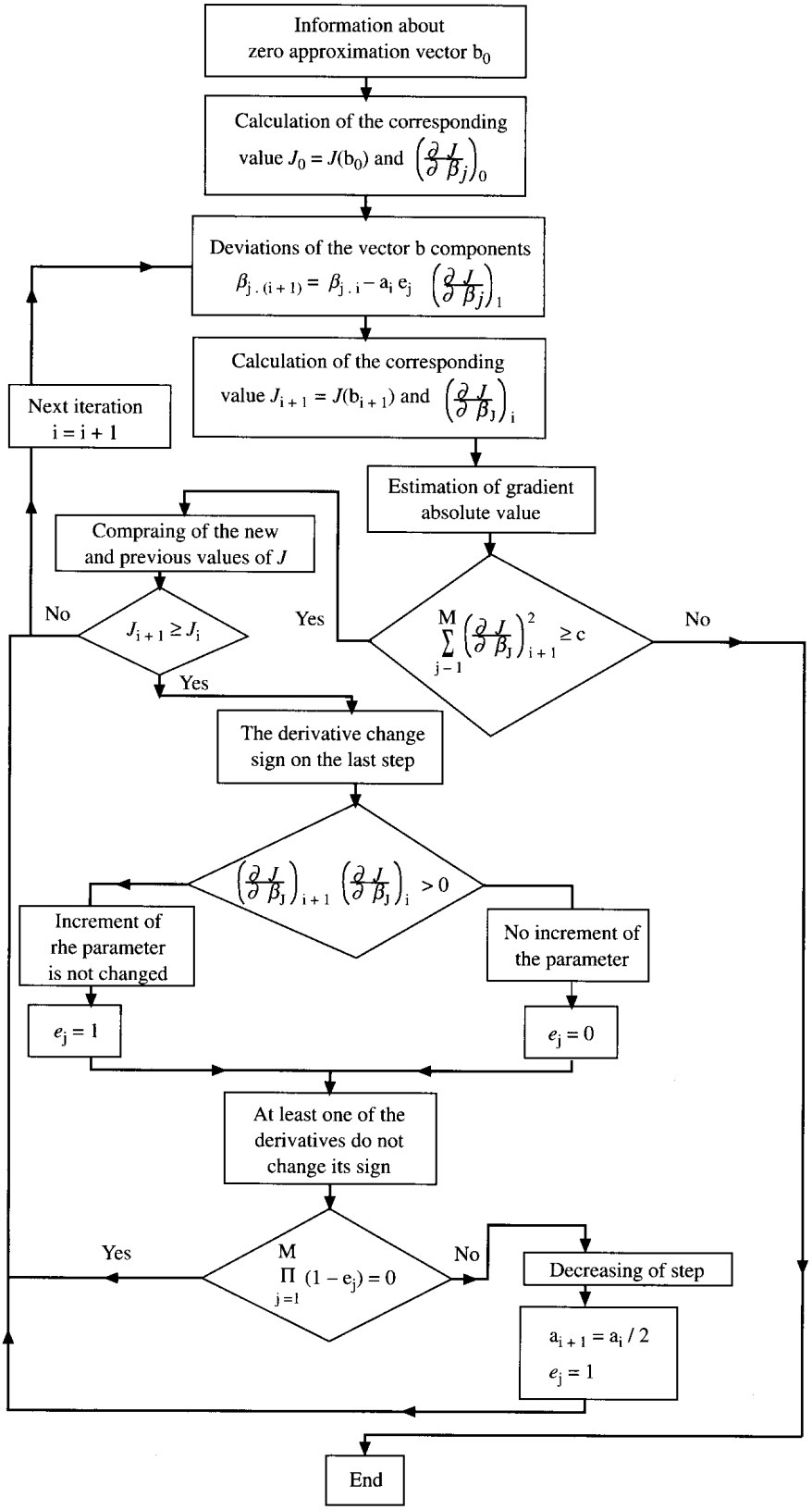


*Fig. 4. A flow chart of the direct identification procedure algorithm*

We did not succeed in using the Gaussian procedure to solve the six parameter model owing to problems of divergence. Instead, we developed an algorithm which performs a direct search for vector b that provides a minimal value of the functional $J$ (Eqn 5). The flow chart of this algorithm is presented as Fig. 4.

The search for a vector b that provides a minimal value of the functional $J$ is performed over a surface $J$ in the six-dimensional space $\{\beta_j\}$. Starting from $J_0$ that corresponds to the zero approximation value $b_0$, the algorithm advances over a path which provides after each step a new value of $J$ smalller than the previous one. The direction of advancement in the $\beta$ plane which provides the quickest decrease in $J$ coincides with the projection of the vector gradient of $J$ on the $\beta$ phase (all $e_j = 1$ in the flow chart).

To achieve this, at each step, the new value of each parameter $\beta_i$ is calculated by adding to the previous value an increment proportional to the derivative $\frac{\partial J}{\partial \beta_j}$. After each step, the program compares new and old values of $J$. When the new value of $J$ is less than the old one, the program makes a new step as described above. Opposite cases in which $J_{i+1} > J_i$ may appear when one or several derivatives $\frac{\partial J}{\partial \beta_j}$ change their sign over the step.

In these cases, the program returns to the previous point and makes a new step in which the corresponding deviations are excluded ($e_j = 0$ in the flow chart). When all derivatives change sign over a step, the program reduces uniformly all components of the step (reducing $a_i$ in the flow chart). The program repeats this procedure until it finds the point where the functional value is less than the previous one. Then the program makes a new step. The procedure ends when the functional gradient absolute value becomes less than some small quantity $\varepsilon$

$$S \equiv \left( \sum_{i=1}^{M} \left( \frac{\partial J}{\partial \beta_i} \right)^2 \right)^{1/2} \leqslant \varepsilon$$

As a final result we get a set of six parameters which provides a minimal value of the functional $J$. Then, using this set and the method described later in Section 4, the evolution of earth surface temperature may be determined. This technique will be acknowledged later in the text as the "direct identification procedure".

## 4. Approximate solution of the radiative cooling problem

In order to implement the minimization procedure for the functional, Eqn (5), it is necessary to express the function $T_s(b, \tau)$ in an analytical form, from which the sensitivity coefficients $X_j$ may be derived. Since there is no exact analytical solution of the heat transfer problem [Eqns (1–4)], we seek an approximate analytical solution.

This solution is obtained by using the heat-balance integral method.[12,13] According to this method, consider that night radiative cooling induces a perturbation in the soil temperature profile which is confined to a layer of thickness $R(\tau)$. The value of $R$ depends only on the time elapsed since the perturbation, and on the heat diffusivity of the soil[13]

$$R(\tau) = \sqrt{6\kappa_g(\tau - \tau_0)} \tag{12}$$

We assume that the temperature profile inside the perturbation zone has a second order form

$$T_g(x, \tau) = a_0 + a_1 x + a_2 x^2 \tag{13}$$

where the unknown coefficients $a_i$ are determined by applying the boundary conditions at the earth surface, Eqn (4), and at the bottom of the heat perturbation zone

$$T_g = T_0 \quad \text{at} \quad x = R(\tau) \tag{14}$$

$$\frac{\partial T_g}{\partial x} = 0 \quad \text{at} \quad x = R(\tau) \tag{15}$$

By substituting Eqn (13) into Eqns (4), (14) and (15), and by taking into account that earth surface temperature in accordance with Eqn (13) is

$$T_s = T_g(0, \tau) = a_0 \tag{16}$$

we obtain a fourth order equation for $T_s$

$$u^4 + qu - r = 0 \tag{17}$$

where

$$u = T_s + 273; \quad q = \frac{2\lambda_g}{\sigma R}; \quad r = q\tilde{T}_0 + \tilde{T}_A^4(A - B \times 10^{-\gamma p})$$

The solution of Eqn (17) (Ref. 14) is

$$T_s = \left( \frac{r}{12v^2} \right)^{1/4} ((2\sqrt{1 + v + v^2} + v^2 - 1)^{1/2} - \sqrt{1 - v^2}) - 273 \tag{18}$$

where

$$v = (\sqrt{w^2 + 1} - w)^{1/3}; \quad w = \frac{q^2}{2}\left( \frac{3}{4r} \right)^{3/2}$$

The comparison of the approximate analytical solution of Eqn (18) with the numerical solution of the problem under consideration [Eqns (1) to (4)] that was described in Ref. 10 is demonstrated in *Fig. 5*. The calculations were carried out for the input data: $T_0 = T_A = 10°C$; $\lambda_g = 1{\cdot}67$ W/mK; $\kappa_g = 8{\cdot}87 \times 10^{-7}$ m$^2$/s; $p = 2{\cdot}4$ mm Hg.

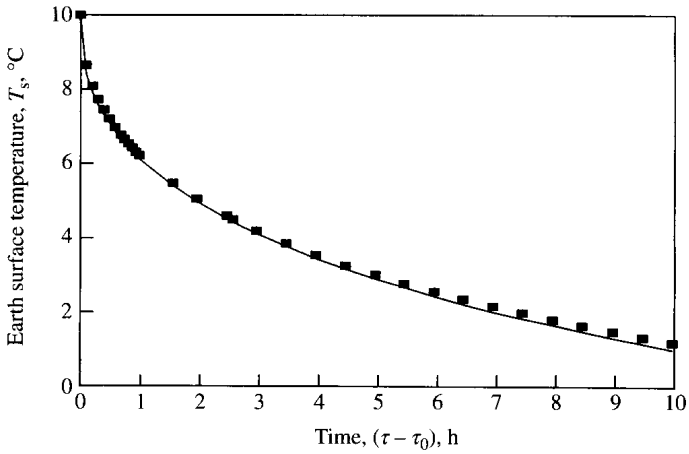


*Fig. 5. A comparison between the numerical (—) (Ref. 10) and the approximate analytical (■) solution (Eqn (18))*

As shown, both solutions are close together, and the difference between the earth surface temperature values at the end of night ($\tau = 8$–$10$ h) is lower than 0·2°C.

Using Eqn (18) we can obtain the sensitivity coefficients $X_j$, to be used in the identification procedure [Eqns (7) to (10)]. Eqn (18) may also be used to calculate the evolution of the earth surface temperature once the values of the parameters are known.

## 5. Results and discussion

Two computer programs were developed on the basis of the above-described algorithms for the Gaussian and the direct identification procedures. The capability of the programs for forecasting temperatures during a night of frost was tested by several numerical experiments.

At first, a simulation of the evolution of earth surface temperature $T_{st}(\tau)$ with time during a night of frost was obtained by means of a numerical solution of Eqns (1) to (4) for the following set of parameters (the "true parameters"): $T_0 = T_A = 10$°C; $\lambda_g = 1{\cdot}67$ W/mK; $\kappa_g = 8{\cdot}87 \times 10^{-7}$ m$^2$/s; $p = 1{\cdot}0$ mm Hg; $\tau_0 = 2000$ h. The resulting temperature profile is described as "true temperature" and is shown in *Fig. 6* by a solid line. Note, in the plot of Fig. 6 that the "true" earth surface temperature falls to 0°C at time $\tau = \tau_1 = \tau_0 + 7{\cdot}72$ h.

Then, for demonstration of the Gaussian identification procedure, a set of ten values of the true temperature $T_{st}(\tau_i)$ from the time interval $[\tau_0, \tau_L]$ (Table 1) was chosen to simulate measured data, $\phi_{ni}$, from which, the Gaussian identification procedure provides the values of the unknown parameters (the "evaluated parameters").

In the next step, the evaluated parameters, which are solutions of Eqn (10), are introduced into the equation set (Eqns (1) to (4)) in order to forecast the earth surface $T_s(\tau)$, during the rest of the night (at times $\tau \geq \tau_L$). Note, that the calculation of the forecast temperatures was accomplished ignoring the values of the true parameters. The only use of the true parameters was to simulate the "measured" set of earth surface temperature $\phi_{n,i}$.

For the five-parameter case, an arbitrary zero approximation vector ($b_0$) was chosen to be: $T_0 = T_A = 15$°C; $\lambda_g = 2{\cdot}5$ W/m K; $\kappa_g = 1{\cdot}33 \times 10^{-6}$m$^2$/s; $p = 0{\cdot}8$ mm Hg.

The result of the Gaussian identification procedure is the vector of the evaluated parameters $b_e$ with the following components: $T_0 = 9{\cdot}6$°C; $T_A = 0{\cdot}1$°C; $\lambda_g = 1{\cdot}98$ W/mK; $\kappa_g = 7{\cdot}61 \times 10^{-7}$m$^2$/s; $p = 1{\cdot}44$ mm Hg. Using these parameters, and Eqn (18), earth surface temperatures were predicted for the time interval $[\tau_L, \tau_f]$. They are shown in *Fig. 6* by filled squares. As shown, the forecast temperature values closely coincide with the "true temperature". The forecasted value $\tau_f$ deviates from the true one by about 20 min.

For comparison, the results for the earth surface temperature, calculated based on the zero approximation $b_0$ are plotted in *Fig. 6* by filled triangles. In this case the result is a large discrepancy between the predicted and the "true" parameters.

It is interesting to note that good agreement between the predicted and the earth surface temperature profiles, is obtained in spite of the rather poor agreement between some of the predicted parameters and the true ones. For example, a true value $p = 1$ mm Hg versus an evaluated $p = 1{\cdot}44$ mm Hg, or a true value $T_A = 10$°C versus an evaluated $T_A = 0{\cdot}1$°C. One may suggest that these parameters have little

**Table 1**
**The set of the earth surface temperature values**

| | | | | | |
|---|---|---|---|---|---|
| Time, h : min | 20:06 | 20:12 | 20:18 | 20:30 | 20:45 |
| Temperature, °C | 8·08 | 7·81 | 7·33 | 6·78 | 6·12 |
| Time, h:min | 21:00 | 21:16 | 21:27 | 21:40 | 21:58 |
| Temperature, °C | 5·54 | 5·07 | 4·70 | 4·41 | 4·08 |

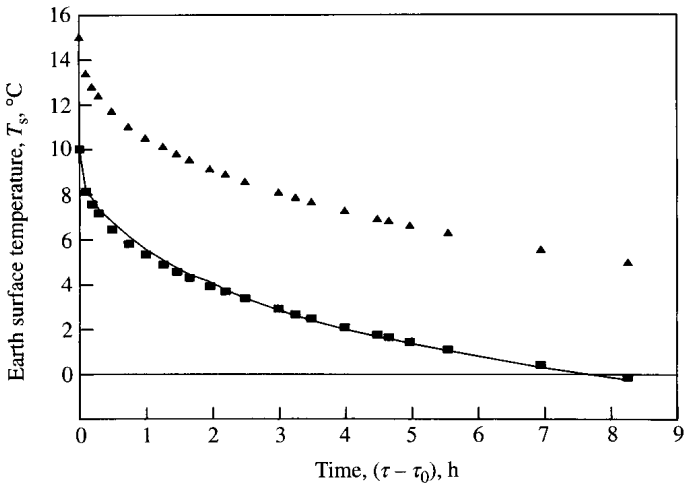


*Fig. 6. Results of the forecast of earth surface temperature during a night of frost (Gaussian identification procedure) —, true temperature; ■; presented method; ▲, zero-approximation*

influence on the effectiveness of predicting $\tau_f$. This suggestion was tested in the following numerical experiment. Eqns (1) to (4) were solved for a set of parameters comprised of four true parameters and the fifth parameter, $p = 1{\cdot}44$ mm Hg. In this case, the discrepancy between the true and the forecast temperatures is much larger and the error in determination of $\tau_f$ reached an extremely high value of 170 min. Similar discrepancies were obtained for other parameters as well.

In a different numerical test, we tested the dependence of the results on the choice of the zero approximation vector, $b_0$. Here, the following set of parameters, $T_0 = 13°C$; $T_A = 16°C$; $\lambda_g = 2{\cdot}84$ W/mK; $\kappa_g = 1{\cdot}15 \times 10^{-6}$ m$^2$/s; $p = 1{\cdot}5$ mm Hg was chosen for a zero approximation. The Gaussian identification procedure yielded the parameter vector $b_e$ with the components: $T_0 = 9{\cdot}6°C$; $T_A = 7{\cdot}1°C$; $\lambda_g = 1{\cdot}46$ W/mK; $\kappa_g = 4{\cdot}04 \times 10^{-7}$ m$^2$/s; $p = 0{\cdot}30$ mm Hg. Although these parameters deviate substantially both from the previous set of evaluated parameters and from the true ones, the predicted earth surface temperature, coincides closely with the true temperature and the $\tau_f$ deviates from the true value by about 6 min.

We conclude that the error in predicting $\tau_f$ is very sensitive to the deviation of each parameter from its true value. However, many combinations of parameters, significantly different from the true values, can provide the required accuracy in forecasting frost conditions.

The direct identification procedure for the six-parameter model, which was described above, was tested for the same true data. For the zero approximation, we assumed the following set of parameters: $T_0 = 8°C$; $T_A = 8°C$; $\lambda_g = 2{\cdot}5$ W/mK; $\kappa_g = 1{\cdot}33 \times 10^{-6}$ m$^2$/s; $p = 1{\cdot}5$ mm Hg; $\tau_0 = 16{\cdot}00$ h.

Note that in contrast with the five-parameter case, here the true value of $\tau_0$ is not given.

Using the developed program, six parameters were identified ($T_0 = 9{\cdot}83°C$; $T_A = 7{\cdot}94°C$; $\lambda_g = 2{\cdot}35$ W/mK; $\kappa_g = 1{\cdot}59 \times 10^{-6}$ m$^2$/s; $p = 1{\cdot}16$ mm Hg; $\tau_0 = 19{\cdot}98$ h) and employed for calculating the temperature distribution in the time interval $\tau_L \leqslant \tau \leqslant \tau_f$. As shown in *Fig. 7*, good agreement with the true temperature distribution (solid line) was obtained and the error in predicting the value of $\tau_f$ is about 24 min.

The main features that were found for the five-parameter case, characterize also the six-parameter case.

Hence numerical experiments showed the good accuracy of the developed techniques in conditions where reality is substituted by its mathematical model. However, the final estimation of the applicability of the techniques may be done only on the basis of field experiments.

## 6. Conclusions

The technique presented in this study uses temperatures measured at the beginning of a night in order to predict temperature evolution during the rest of the night. The method is applicable when radiative frost conditions (no wind, cloudless) prevail during the whole night.

Good accuracy of the presented method was demonstrated by comparing the predicted temperatures with temperatures obtained by solving a deterministic problem.

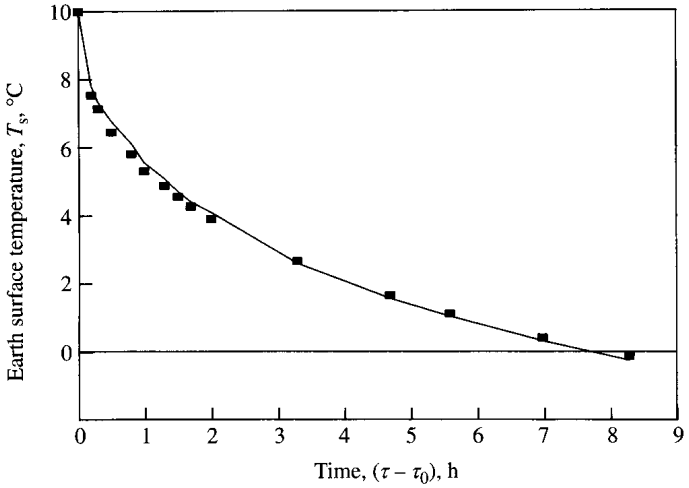


*Fig. 7. Results of the forecast of earth surface temperature during a night of frost (direct identification procedure). —, true temperature; ■, forecast*

Our technique determines uniquely and adequately the evolution of earth surface temperature for the rest of a night of frost from a given set of earth surface temperatures, measured over some time interval at the beginning of the night. There is no unique relationship between the set of measured temperatures and the values of governing parameters. Different sets of derived parameters may in fact be associated with satisfactory prediction of earth surface temperature.

An analytical solution of the heat transfer problem, which was originally developed for implementation of the identification procedures, coincides well with the numerical solution.

Field experiments during a night of frost are still required for verification of the applicability of the developed technique.

## Acknowledgement

This research was supported by the Israel Ministry of Absorption, Ministry of Energy and the Fund for the Promotion of Research at the Technion, Israel Institute of Technology. We are grateful for this help.

## References

[1] **Sutcliffe J F** Plants and Temperature. London: Arnold, 1977

[2] **Gates D M** Heat transfer in plants. Scientific American, 1965, **213**(6): 76–84

[3] **Barfield B J; Gerber J F** Modification of the Aerial Environment of Plants. ASAE; St. Joseph, 1979

[4] **Braud H J; Jerry L C** Physical properties of foam for protecting plants against cold weather. Transactions of American Society of Agricultural Engineers, 1970, **13:** 1–5

[5] **Brooks F A** An Introduction to Physical Microclimatology. Davis Campus University of California 1959

[6] **Stombaugh T S; Heineman P H; Morrow C T; Golart B L** Automation of a pulsed irrigation system for a frost protection of strawberries. Applied Engineering in Agriculture, 1992, **8**(5): 597–602

[7] **Geiger R** The Climate Near the Ground. Cambridge, USA: Harvard University Press 1966

[8] **Angström A** Uber die Gegenstrahlung der Atmosphäre. [On reflection by the atmosphere]. Meteorologische Zeitschrift 1916, **33:** 529–538 (in German)

[9] **Bolz H M; Falckenberg G** Neubestimmung der Konstanten der Angströmschen Strahlungsformel. [Redetermination of the constants of the Angstrom radiation formula.] Zeitschrift für Meteorologie. 1949, **3:** 97–100 (in German)

[10] **Krasovitski B: Kimmel E; Amir I** A simulation of foam protection of plants against frost, 1995, **61:** 155–163

[11] **Beck J V; Arnold K J** Parameter estimation in engineering and science. Wiley, 1977

[12] **Goodman J** The heat balance integral and its application to problem involving change of phase. Transactions of the American Society of Mechanical Engineers, 1958: **80:** 335–342

[13] **Dubina M M; Krasovitski B A; Lozovski A S; Popov F S** Teplovoe i mehanicheskoe vzaimodejstvie injenernyh soorujenij s merzlymi gruntami (Heat and Mechanical Interaction between Structures and Frozen Ground]. Publishing House "Nauka", Siberian branch, Novosibirsk, 1977. (in Russian)

[14] The Universal Encylopedia of Mathematics. New York: Simon and Schuster, 1964